The impact of radiative forcing on the equatorial stratospheric circulation

Author: Aleksander Lacima Nadolnik*
Facultad de Física, Universidad de Barcelona, Av. Diagonal 647, 08028 Barcelona, España.

Supervisors: Froila Palmeiro Núñez and Javier García Serrano†

Abstract: The aim of this work is to evaluate how the Quasi-Biennial Oscillation (QBO), which dominates interannual variability in the tropical stratosphere, responds to different radiative forcings in the EC-EARTH climate model version 3.3. Two sets of simulations have been used, consisting in three atmosphere-only and three atmosphere-ocean coupled experiments, which are based on past, present and future conditions. The QBO influence on the extratropical circulation, formally known as the Holton-Tan effect, has also been assessed during boreal winter (DJF). Results show a notorious shortening of the QBO period and a clear weakening of the QBO amplitude under a warming climate in the coupled simulations; which do not show a significant impact on the Holton-Tan effect in the polar vortex.

I. INTRODUCTION

The Quasi-Biennial Oscillation (QBO) is the dominant mode of climate variability in the equatorial stratosphere, roughly extending between 5 and 100 hPa. The QBO can be visualized as a shifting pattern of easterly and westerly winds that propagate downward with a period ranging from 22 to 34 months, hence the name quasi-biennial, and a mean period of 28 months. On average, this downward propagation takes place without loss of amplitude in the upper stratosphere, though it rapidly dampens below 20 hPa (23 km). A complete QBO cycle is then composed of an easterly (EQBO) and a westerly phase (WQBO), with the former usually having a greater amplitude, in absolute terms, and the latter usually propagating downward at a higher rate. The QBO extends symmetrically across the equator, approximately between 6°N and 6°S, and around the entire equatorial belt (*Baldwin* 2001).

From a dynamical perspective, the QBO is driven by upward propagating equatorial waves that arise in the troposphere at tropical latitudes. In general terms, atmospheric waves can only propagate vertically when their frequency, ν, satisfies the condition $f < \nu < N$, where f is the Coriolis parameter and N is the buoyancy frequency. This constraint implies that in mid-latitudes most waves with periods in the order of days (low-frequency waves) are vertically trapped, thus only being capable of propagating horizontally. But at equatorial latitudes, where f tends to 0, low-frequency waves can propagate vertically. Thus, equatorial waves, which include gravity, inertia-gravity, Kelvin and Rossby-gravity (R-g) waves (also known as Yanai waves), interact with the mean flow by depositing energy, mainly in the form of heat, and momentum, $\overline{u'w'}$, in the upper stratosphere, where they develop an alternating pattern of wind regimes that propagates downward at a rate of approximately 1 km per month, until it dissipates in the tropical tropopause (TPP). This deposition of energy and momentum occurs due to wavebreaking, a process through which waves dissipate when their phase speed reaches a critical value (i.e. the zonal wind speed). Both Kelvin (eastward propagating) and R-g (westward propagating) waves originate due to oscillations in the large-scale convective heating pattern present around the equatorial belt and are also equatorially trapped, meaning that they rapidly decay away from the equator (*Holton and Hakim* 2012).

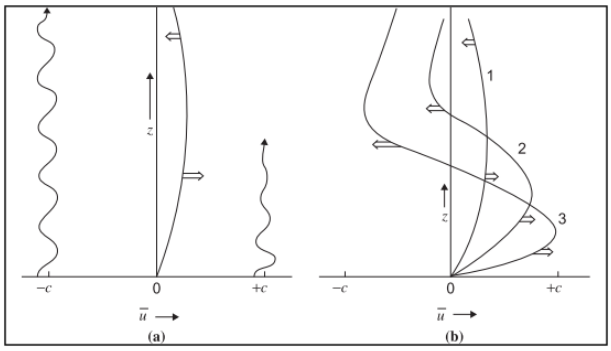

FIG. 1. Schematic representation of the wave-driven development of a QBO cycle. Source: *An Introduction to Dynamic Meteorology, Holton, 2012.*

The wave-driven development of a QBO cycle is schematically depicted in Figure 1b. Initially (1), the zonal wind is weak and westerly, with a small amplitude maximum located at mid-altitude. Kelvin waves propagate upward until they reach this maximum, where they dissipate and force a westerly acceleration on the mean flow. As the westerlies intensify due to this forcing they advance downward in time, thus lowering the altitude at which Kelvin waves break (2). At the same time, R-g waves propagate to higher altitudes as they are not trapped by the westerly maximum at middle levels. Therefore, they force an easterly acceleration on the mean flow right

* alekslacima@gmail.com
† fm.palmeiro@meteo.ub.edu; j.garcia-serrano@meteo.ub.edu

above the westerly region, developing easterly winds that also progress downward in time. This process continues until the lower phase reaches the TPP and dissipates, leaving the lower and mid stratosphere dominated by easterlies (3). At this point the cycle restarts again, but this time with the westerly phase aloft.

It has been observed that equatorial waves provide a significant fraction of the vertical momentum flux needed to drive the QBO. More specifically, Kelvin waves (which have no meridional component, $v' = 0$) transport westerly momentum, $\overline{u'w'} > 0$, into the stratosphere, thus providing a zonal momentum source for the QBO to develop its westerly phase. On the other hand, R-g waves also present a positive vertical westerly momentum flux, $\overline{u'w'} > 0$, but their total impact on the mean flow cannot be solely determined by this vertical flux, as a strong meridional component, v', is also present. R-g waves thus present a strong poleward heat flux, $\overline{v'T'} > 0$, which implies that the vertical component of the Eliassen-Palm flux is non-zero:

$$F_z = \rho_0 f_0 R\overline{v'T'}/(N^2 H) \tag{1}$$

Where ρ_0 is the reference air density, f_0 is the reference Coriolis parameter, N is the buoyancy frequency, H is the scale height and R is the gas constant for dry air. F_z dominates over $\overline{u'w'}$ resulting in a net transport of easterly momentum flux by R-g waves into the stratosphere, thus providing a zonal momentum source for the QBO to develop its easterly phase. Even so, measured momentum fluxes due to Kelvin and R-g waves are not enough to account for the observed zonal accelerations of the QBO. The rest of the required momentum flux is provided by smaller scale waves generated by convective storms, such as gravity and inertia-gravity waves (*Holton and Hakim* 2012).

Even though the QBO is a phenomenon confined to the equatorial stratosphere, it affects the entire stratospheric circulation by playing a key role in the transport of trace constituents (e.g. O_3, CH_4, H_2O) in the lower stratosphere, where it modifies the variability of the Brewer-Dobson Circulation (BDC) through its secondary meridional circulation (Fig. 2). During a WQBO phase a westerly shear zone emerges just below the descending westerly winds where air sinks, $w < 0$, thus weakening tropical upwelling and favoring the meridional component of the BDC in the lower stratosphere, allowing constituents to enter the so called *surf zone*, one of the four regions in which the stratosphere is usually divided, at lower altitudes. Oppositely, during the EQBO phase an easterly shear zone appears beneath the descending easterly winds where air rises, $w > 0$, thus strengthening tropical upwelling and reinforcing the vertical component of the BDC (*tropical pipe*), which forces constituents to ascend higher before being able to drift poleward (*Plumb* 1996; *Flury et al.* 2013; *Butchart* 2014).

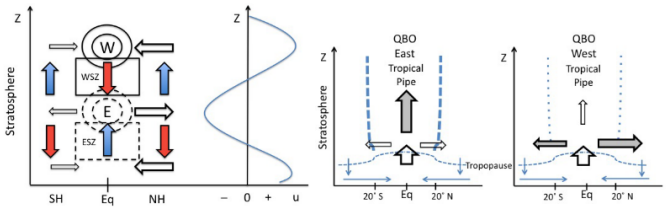

FIG. 2. Schematic representation of the QBO secondary meridional circulation and its effects on the variability of the Brewer-Dobson Circulation. Source: *Flury et al.* 2013

The QBO also exerts a significant influence on high latitudes, well above 30°, by modulating the propagation of extratropical waves. Through this modulating mechanism the QBO can contribute to the disruption of the winter stratospheric polar vortex. As the vortex heavily affects weather patterns in the troposphere, mainly through changes in the variability of the North Atlantic Oscillation (in the NH), this provides a pathway for the QBO to exert its limited but relevant influence even at the lowest tropospheric levels. More specifically, when the QBO is in its easterly phase (EQBO) it can cause Rossby planetary waves to deflect poleward, thus weakening the polar vortex, whereas in its westerly phase (WQBO) Rossby waves tend to get deflected equatorward, therefore strengthening the vortex. The influence of the QBO on the extratropical atmospheric circulation is widely known as the Holton-Tan effect (*Holton and Tan* 1980; *Anstey and Shepherd* 2014; *Palmeiro et al.* 2020).

The QBO has been usually regarded as a feature of climate variability which could be employed to improve the predictability of global climate models (GCMs), as its period of oscillation was deemed to be one of the most regular climatic phenomenons since its discovery in the late 1950s. However, this apparent robustness has been recently questioned as the QBO cycle was disrupted during the boreal winter season of both 2015/2016 and 2019/2020, when the incipient transition from a WQBO to an EQBO phase was interrupted by the appearance of westerly winds above the 30-hPa level, therefore effectively destroying the EQBO phase that would have emerged under usual circumstances (*Osprey et al.* 2016; *Anstey et al.* 2020). From a dynamical perspective, disruptions may occur when large horizontal fluxes of momentum (meridional EP fluxes), $\overline{u'v'}$, intrude into the equatorial region from higher latitudes. The classical dynamic description of the QBO accounts only for the interaction of the mean flow with upward propagating equatorial waves, while considering meridional fluxes of momentum coming from extratropical latitudes as negligible when compared to vertical fluxes originating in the tropics.

Anstey et al. (2021) suggest that the 15/16 wintertime disruption occurred due to an usually large horizontal flux of momentum coming from higher latitudes in the NH, which arose from a very strong ENSO event. On the contrary, in the 19/20 disruption the meridional EP flux originated in the SH, due to a change in the meridional circulation caused by a minor sudden stratospheric warming (SSW). Futhermore, under a warming climate scenario these meridional EP fluxes are expected to intensify, so that equatorward propagating waves would be theoretically capable of affecting the QBO and therefore lead to an increase in the number of disruptions. If climate change causes the QBO to be more easily and frequently disrupted this will have a direct impact on the predictive capabilities of GCMs (*Anstey et al.* 2021).

This work aims to investigate how variations in the radiative forcing affect the simulated equatorial stratospheric circulation in a global climate model and to explore how these changes may modify the QBO influence on the extratropical circulation. The different outcomes of using atmosphere-only and coupled simulations are also considered.

II. DATA & METHODOLOGY

In this section we briefly describe the climate model and the analyzed fields (Subsect. A), and also provide details on the different methodologies employed for the data analysis (Subsect. B).

A. DATA

The data used in this work come from simulations performed with the EC-EARTH climate model version 3.3. EC-EARTH is a global coupled model that includes several components of the climate system. It is based on the Integrated Forecast System (IFS) atmosphere model, cycle 36r4 in EC-EARTH3.3, developed at the European Centre for Medium-Range Weather Forecasts (ECMWF), coupled to the Nucleus for European Modelling of the Ocean (NEMO) ocean model, version 3.6 in EC-EARTH3.3. Details about the model and its components can be found in *Döscher et al.* (2021). The standard configuration of IFS in EC-EARTH3.3 (hereafter, EC-EARTH) is at horizontal spectral resolution T255 (triangular truncation at wavenumber 255), corresponding to 0.7° in longitude-latitude (∼80 km), with 91 vertical levels up to 0.01 hPa (L91). Two types of simulations (hereafter, 'families') have been analyzed: *atmosphere-only simulations* (ATM), where sea surface temperature (SST) and sea ice concentration (SIC) are prescribed according to the observed climatology over 1988-2007, following the setup in QBOi from SPARC (Stratosphere-troposphere Processes And their Role in Climate; *Butchart et al.* 2018), using SST/SIC provided by CMIP6 - Coupled Model Intercomparison Project phase 6; and atmosphere-ocean *coupled simulations* (CPL), where the ocean is allowed to vary according to its interaction with the atmosphere. Three experiments have been analyzed for each family of simulations, where the radiative forcing is kept fixed along the integration, including: well-mixed greenhouse gases (e.g. CO_2, CH_4, $CFCs$, N_2O), aerosols, stratospheric ozone and solar insolation. The three experiments are representative of 'past' (fixed at 1950), 'present' (fixed at 2000) and 'future' (fixed at 2050) climate conditions, with the radiative forcing provided by CMIP6 according to observational estimates for the historical scenarios (1950, 2000) and projected values of the Shared Socioeconomic Pathway (SSP) 2-4.5 for the future scenario (2050). It is important to remark that the differences between radiative forcings are not linear, thus when evaluating the differences between 'past', 'present' and 'future' linear responses should not be expected as a result. The six simulations, three experiments per family, consist of 250 years after spin-up, namely a period of time needed for the simulation to stabilize and approximately reach a steady state. Note that this stationary state, not following transient, time-evolving conditions, does not necessarily apply to the deep ocean which would probably drift for thousand of years.

The QBO has been characterized using monthly-mean values of zonal-mean wind, $\overline{U}$, meridionally averaged over 5°S and 5°N, for 28 vertical pressure levels ranging from 1000 hPa, at the surface, to 1 hPa, at the stratopause (STP). As the QBO is a purely stratospheric phenomenon it is entirely encompassed between 100 and 1 hPa, which at equatorial latitudes equates roughly to an altitude spanning from 16 to 50 km. Figures 3 and 4 display the initial QBO cycles for each family of experiments. Complete figures containing all the cycles for the 250-year period are not shown, though they behave similarly to the initial ones shown in the aforementioned figures. $\overline{U}$ data, as a function of latitude, has also been employed to assess the Holton-Tan effect on the extratropical stratosphere.

Other fields have been extracted and analyzed, including: total precipitation (TP), air temperature (T), and geopotential height (Z), for both families of experiments, ATM and CPL; while SST has only been diagnosed for CPL, as this field is prescribed in ATM.

B. METHODOLOGY

The QBO can be characterized in different ways, being its amplitude (maximum/minimum wind speed) at a certain pressure level and its period of oscillation, (complete cycle of EQBO and WQBO phases) the key metrics. In this work we have mainly focused on the latter, as it allows for a more robust characterization of the QBO, though amplitudes have also been examined. The period offers

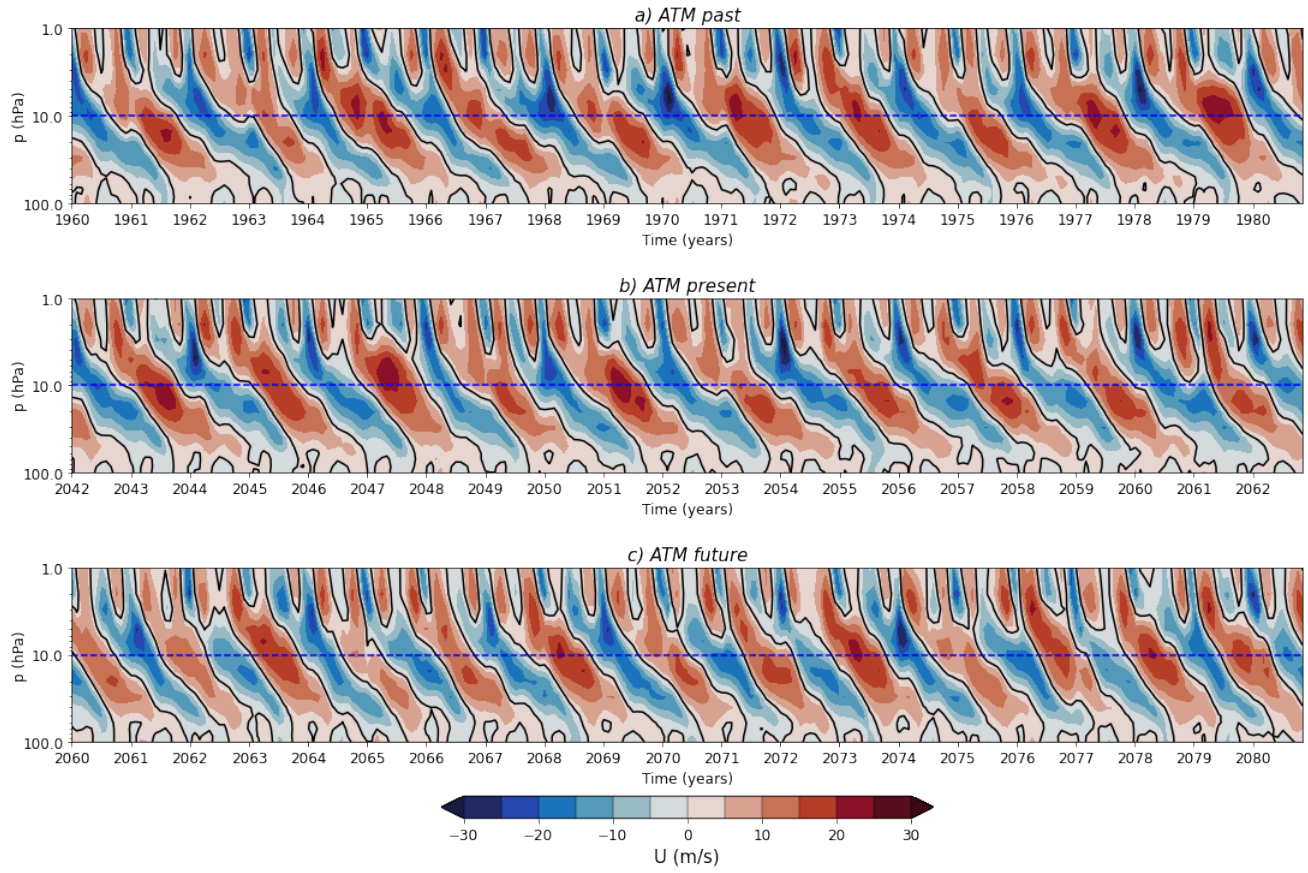

FIG. 3. Initial QBO cycles in EC-EARTH atmosphere-only simulations for (a) past, (b) present and (c) future radiative forcing. Red and blue shading (every 5 ms^{-1}) represents westerly (eastward) and easterly (westward) winds, respectively. The blue horizontal dashed line indicates the pressure level of 10 hPa. The black solid contour stands for 0 ms^{-1} wind speed.

a slightly more robust characterization as it barely varies when modifying the latitudinal extension used to define the QBO. On the contrary, amplitude tends to weaken as the meridional range of definition is extended, due to weakening of the stratospheric zonal wind away from the equator. Additionally, $\overline{U}$ has also been deseasonalized for the sake of a better graphical representation.

Obtaining the QBO period may appear simple at first, considering that it is a periodic oscillation, but the pattern structure of the descending winds varies strongly with time and height, therefore making the calculation of the period to be relatively complex. The approach followed by *Richter et al.* (2020) is adopted in this work. Precise times of transition from EQBO to WQBO and from WQBO to EQBO phases are obtained from the meridionally-averaged zonal-mean zonal wind time series at 10 hPa. The QBO period is then defined as the difference in successive transition times between phases of the same sign; hence, two estimates of the QBO period are obtained, T_{EQBO} and T_{WQBO}. Finally, the average of both estimates, based on the two wind regimes of each QBO cycle, is calculated (T_{QBO}), thus providing a more robust estimate of the QBO period:

$$T_{QBO} = \frac{1}{2}(T_{EQBO} + T_{WQBO}) \tag{2}$$

This two-step calculation, combined with a thorough visual inspection of all the QBO cycles, was required in order to eliminate several outlier values that inherently appear in the transition method. Moreover, it is worth noting that no pressure level is widely accepted in the literature as the most suitable to characterize the QBO. For this reason, studies usually characterize it by selecting the pressure level where the amplitude is the greatest, even though amplitude can vary with height from one QBO cycle to another, or the level where a certain signal response, used to evaluate QBO teleconnections with other atmospheric levels/regions, is the most intense.

QBO amplitude has also been analyzed as it can provide some insight on whether the wind regimes are weakening, strengthening or remaining stable. In order to get as much information as possible, two different approaches have been followed for the amplitude analysis. The first one, and more simple, consists in computing

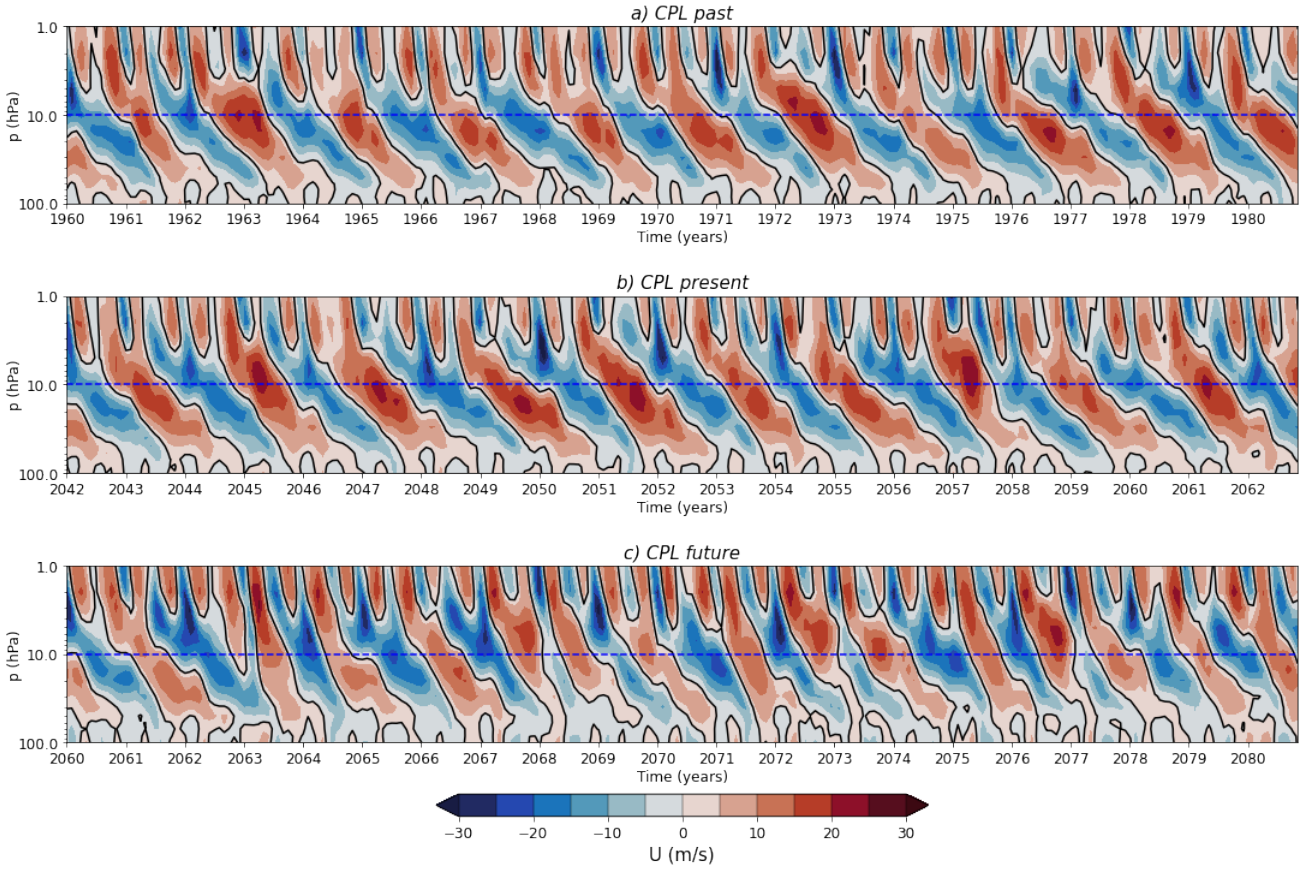

FIG. 4. Initial QBO cycles in EC-EARTH atmosphere-ocean coupled simulations for (a) past, (b) present and (c) future radiative forcing. Red and blue shading (every 5 ms^{-1}) represents westerly (eastward) and easterly (westward) winds, respectively. The blue horizontal dashed line indicates the pressure level of 10 hPa. The black solid contour stands for 0 ms^{-1} wind speed.

the mean amplitude for EQBO and WQBO phases at the 10- and 50-hPa levels. The second approach, slightly more complex, is based on identifying the maximum amplitude for each time instant at any pressure level between 50 and 5 hPa. Two amplitude series are thus obtained, one for each QBO phase, allowing to calculate the mean pressure level at which the maximum amplitude occurs. Variations in amplitude and in the pressure level at which this maximum amplitude occurs provide information on whether the QBO is changing under different radiative forcings.

The analysis of TP, T and SST has been very similar, i.e. comparing differences in the climatological field between experiments. This approach allows to study the effect of increasing radiative forcing, by analysing the differences between experiments of the same family, as well as the effect of ocean coupling, by examining the differences between experiments of different families. In this work we have mainly focused on the former, as assessing the impact of air-sea interaction is out of the scope of this study, and it is left for future analyses. $\overline{U}$ data has also been used to evaluate the Holton-Tan effect on the extratropical stratosphere.

Finally, in order to assess if the obtained results are statistically significant, a t-test for difference of means is used. A two-tailed Welch t-test is performed between pairs of data series. Similarly to Student's t-test, Welch's t-test assumes that the sample's underlying distribution adopts a Gaussian form, but it differs from the former in considering unequal variances between populations. A significance level of $\alpha = 0.01$ has been used.

III. RESULTS & DISCUSSION

A. QBO Period & Amplitude

Performed analyses clearly show that under a warming climate the QBO cycle suffers a marked acceleration (Fig. 5), a behaviour that is more notorious in the CPL family, where the increase in temporal variability is also important, as it can be seen from the increasing spread in the probability density functions (PDFs).
It can be therefore inferred that the coupling with the ocean is the main reason behind the observed increase of variability in the QBO period. In the CPL simulations the number of cycles increases by approximately a 50%

TABLE I. QBO amplitude in m/s.

Experiment	$WQBO_{10}$	$EQBO_{10}$	$WQBO_{50}$	$EQBO_{50}$	$WQBO_m$	$EQBO_m$	$p_{Wlev}(hPa)$	$p_{Elev}(hPa)$
ATM past	7.6	-17.0	4.9	-5.7	8.3	-26.3	24.6	9.7
ATM present	6.5	-17.5	4.9	-4.8	7.9	-26.3	25.8	9.7
ATM future	6.8	-15.4	4.3	-5.6	7.6	-24.8	24.7	9.6
CPL past	6.7	-17.7	5.1	-5.6	7.8	-25.2	25.9	10.7
CPL present	6.7	-17.3	4.8	-4.9	7.9	-25.2	24.8	10.1
CPL future	8.5	-12.6	2.5	-2.4	9.4	-23.3	15.7	6.6

between the past and future experiments, whereas the mean period decreases by 7 months.

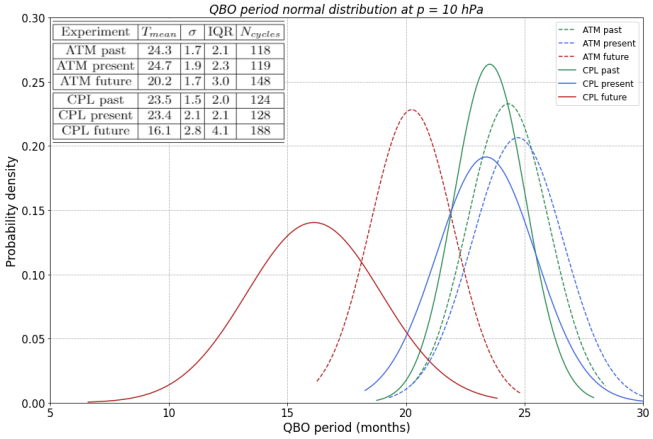

FIG. 5. Probability density functions of the QBO period for three atmosphere-only (ATM) and atmosphere-ocean coupled (CPL) simulations.

On contrast, in the ATM family one can notice that the effect of increased forcing is to moderately accelerate the QBO, while having a negligible impact on its variability. In this case the number of cycles rises roughly a 25%, while the mean period decreases approximately by 4 months. Thus, the coupling with the ocean can also be accounted for further accelerating the QBO with respect to the atmosphere-only simulations.
The differences in mean period that appear in Fig. 5 were found to be statistically significant at the 99% confidence level for all the experiments, with the exception of the differences between present and past, which were found to not be statistically significant for both families of simulations.

The performed analysis on QBO amplitude is condensed in Table I. For the ATM family the mean maximum amplitudes, $WQBO_m$ and $EQBO_m$, and the pressure levels where these amplitudes occur, p_{Wlev} and p_{Elev}, remain generally stable, without showing any significant variations and therefore no signs of weakening or strengthening. As for the CPL family, there are important variations both in amplitude and pressure level between CPL future and the other two experiments. The amplitude of the WQBO phase increases by almost 2 ms^{-1} and the pressure level moves upward from around 25 (31 km) to 16 hPa (35 km). On the other hand, the amplitude of the EQBO phase decreases between 2 and 5 ms^{-1}, depending on the levels considered, whereas the pressure level moves upward from around 10 (39 km) to 7 hPa (42 km), with an increase in height similar to the one observed for the WQBO phase. The rise of the pressure level occurs due to severe weakening of the amplitude at lower levels (around 50 hPa) in CPL future, as both $WQBO_{50}$ and $EQBO_{50}$ suffer a decrease of roughly a 50 %.

Considering the established literature, the most plausible explanation for the observed weakening is increased tropical upwelling, associated to the BDC, in the lower stratosphere. Current climate projections imply that rising sea surface and air temperatures in the tropical troposphere will lead to an increase in deep tropical convection. Under such conditions, equatorial waves would be capable of carrying more energy and momentum upward, thus exerting a more intense wave drag at high (low) tropospheric (stratospheric) levels when breaking. Stronger wave drag leads to enhanced tropical upwelling, which directly opposes the QBO downward progression by effectively dampening its amplitude in the lower stratosphere (*Kawatani and Hamilton* 2013; *Butchart* 2014; *Anstey and Shepherd* 2014).
The amplitude and pressure level differences between ATM experiments were found to not be statistically significant, except for the EQBO amplitude between ATM future and the other two ATM experiments (Table I). On contrast, the difference between CPL future and the other two CPL experiments was found to be statistically significant at the 99 % confidence level for all values.

B. Deep tropical convection

The simplest explanation for an accelerated QBO is increased wave-activity in the equatorial troposphere due to a marked increase in convection. Being so, we expect changes in the TP, SST and T fields at tropical latitudes to give us an explanation for the observed behaviour. There are no remarkable differences in the TP field between present and past simulations (Fig. 6a-b), but there is an important rise in precipitation

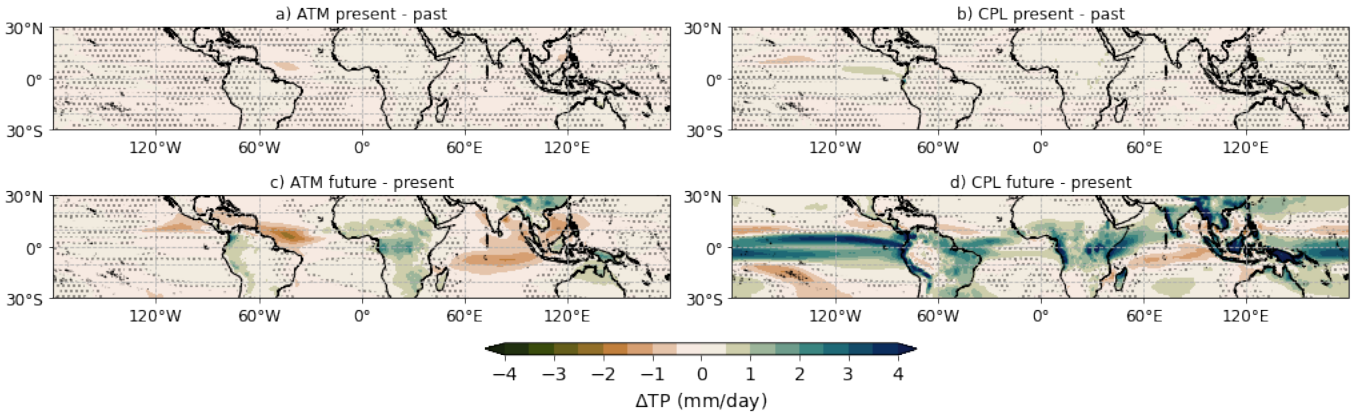

FIG. 6. Difference in annual-mean TP climatology between EC-EARTH simulations of the same family. Blue and brown shading (every 0.5 mm/day) represents positive (wetter) and negative (drier) variations in precipitation, respectively. Dotted areas indicate where the differences are not statistically significant at the 99 % confidence level.

between future and present (Fig. 6c-d).
For the ATM case, the TP increase is almost entirely localized over continental masses, with the highest increments located over Equatorial Africa, South-East Asia and west of the Amazon Basin. The descent in precipitation is concentrated over the oceans, mostly in the Indo-Pacific region and the western Tropical Atlantic (Fig. 6c). Overall, if TP is meridionally averaged for each of the ATM experiments, over 5°N and 5°S, no significant increase in precipitation is found (Fig 13). Therefore, the observed QBO acceleration in ATM future cannot be explained by a rise in equatorial wave-activity linked to enhanced convection in the tropics, as the marginal variations observed in the TP field outrule this mechanism. Being so, other atmospheric processes should be considered to reach a feasible explanation for the observed behaviour, something that unfortunately is out of the scope of this work.

CPL future shows a much steeper increase in TP (Fig. 6d), which is distributed inhomogeniously around the equatorial belt and extends roughly between 10°N and 10°S across the equator, with several regions, like South-East Asia, the North-Eastern Equatorial Pacific, and some parts of Equatorial Africa, presenting a rise of more than 4 mm/day. The impact of the radiative forcing on the TP field is thus much more evident in the CPL case. If TP is again meridionally averaged, similarly as for ATM, a large increment in precipitation is then observed throughout all seasons (Fig. 14). Such vasts increments in precipitation can only be linked to a strong growth in deep tropical convection. Consequently, it can be inferred that the observed QBO acceleration in CPL future is the product of expanded wave-activity in the equatorial troposphere. A feasible explanation that could account for this accelerated downward progression relies on higher numbers of equatorial waves, arising due to increased convection, reaching the stratosphere, thus rising the wavebreaking rate. In other words, a

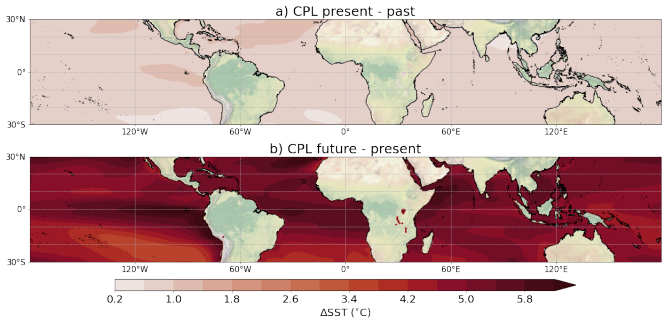

FIG. 7. Differences in annual-mean SST climatology between the EC-EARTH CPL simulations. Red shading (every 0.4 °C) represents increasing temperatures. Dotted areas indicate where the differences are not statistically significant at the 99 % confidence level.

reduction in the time elapsed between the dissipation of successive waves could, according to theory, explain the observed acceleration. However, further studies will be needed to thoroughly assess how this expanded wave-activity actually manifests in reality.

The rise in convection can be easily understood under climate change, which causes rising sea surface and air temperatures (Fig. 7, Fig. 11). Both higher T and SST enhance the evaporation rate while a warmer troposphere is capable of containing more humidity, thus creating suitable conditions for a growth in convection. SSTs are considerably larger in this future scenario (Fig. 7b), with temperature differences surpassing even 5 °C differences in several regions of the tropics. Transpiration from vegetation is not accounted for in EC-EARTH, but it would be interesting to assess how it modifies the observed changes in the TP field, as our analysis is focused in the latitudes where all the tropical rainforests of the planet are localized.

Atmosphere-only simulations in EC-EARTH correctly reproduce the QBO and even partially display the effects caused by a greater radiative forcing, but fail to consistently capture the expected impacts on other fields that would, according to theory, account for the observed acceleration. Thus, it appears that atmosphere-ocean coupling cannot be neglected when trying to understand how the stratospheric circulation changes under a warming climate, as it provides a more realistic workframe. For this reason, the last section of this work focuses only on the CPL experiments, as they have proven to be more reliable in providing an explanation for the obtained results.

C. The future QBO

Considering the established literature, CPL future is probably the experiment that best captures the effects of a warming climate on the QBO (Fig. 4c). It shows a steep acceleration in the QBO cycle that is expected under increased convection and expanded wave-activity, and presents a severely weakened amplitude in the lower stratosphere that is also expected due to intensified tropical upwelling under climate change. Additionally, though it is hard to evaluate thoroughly, CPL future does not outrule the occurrence of QBO disruptions (*Taguchi* 2010; *Kawatani and Hamilton* 2013).

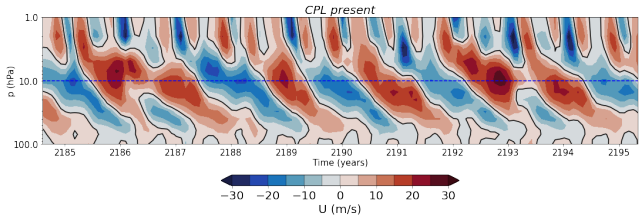

FIG. 8. Two disrupted QBO cycles found in CPL present.

For the EC-EARTH simulations analyzed in this work, disruptions are observed in CPL present and for only 2 QBO cycles from a total of 128 (Fig. 8). These two westerly disruptions occur after nearly 150 years have passed from the start in 2042, and with only two complete QBO cycles between them. Perhaps the most remarkable feature is their mere appearance, as it implies that EC-EARTH (and potentially other GCMs too) is capable of reproducing the occurrence of disruptions, but only in atmosphere-ocean coupled simulations, as disruptions were not observed in the ATM experiments.

The main conclusion to be extracted here is that the interaction between ocean and atmosphere is somehow responsible of either increasing the flux of westerly momentum or reducing the easterly one. A combination of both effects could also be possible, but either way there needs to be at least a relative increase in the westerly momentum flux, as both the real observed disruptions and the EC-EARTH ones are composed of westerly winds. This anomalous increment in $\overline{u'v'}$ is only possible through intrusions of large horizontal fluxes of momentum coming from extratropical latitudes, as Kelvin or other eastward propagating waves would be vertically trapped by the descending WQBO phase (*Anstey et al.* 2021).

D. Holton-Tan effect

Due to the limited nature of this work the assessment of the Holton-Tan effect has only been conducted for the NH, as the results were found to be clearer than in the SH. Composites of zonal-mean zonal wind and geopotential height have been constructed to evaluate how the different radiative forcings affect the QBO influence on the extratropical circulation.

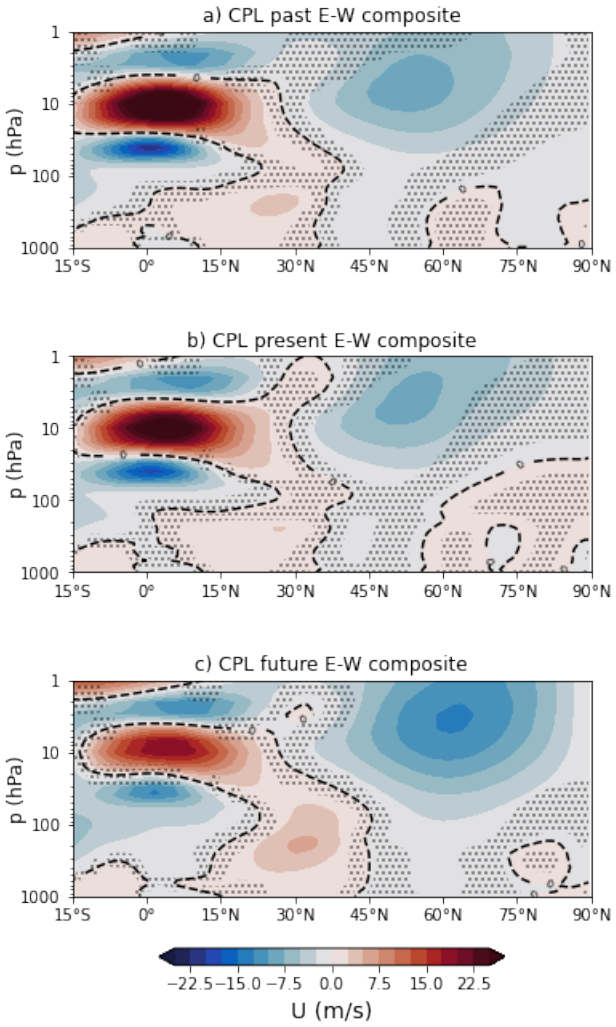

FIG. 9. Vertical cross-section of zonal-mean zonal wind composite difference between EQBO and WQBO phases, identified with $\overline{U}_{EQ50}$, during boreal winter (DJF) for the EC-EARTH CPL simulations. Red and blue shading (every 2.5 ms^{-1}) represents westerly and easterly winds, respectively. Dotted areas indicate where the EQBO-WQBO differences are not statistically significant at the 99 % confidence level. The grey dashed contour stands for a zero difference.

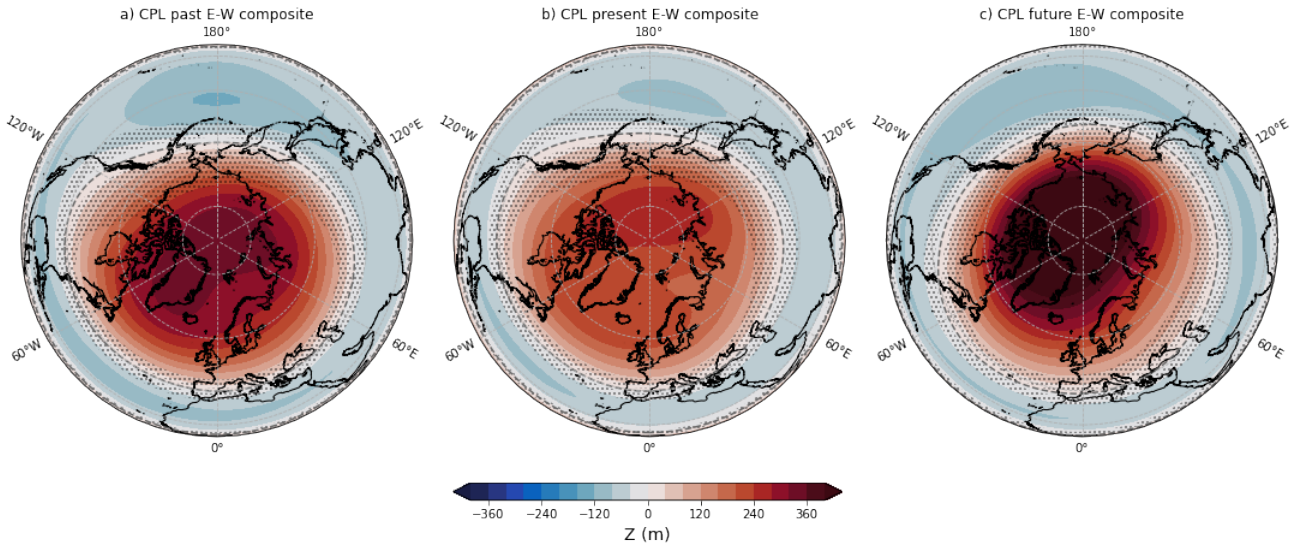

FIG. 10. Difference in geopotential height at 10 hPa for the EQBO-WQBO composite of Fig. 8 in the EC-EARTH CPL simulations during boreal winter (DJF). Red and blue shading (every 40 m) represents positive and negative anomalies, respectively. Dotted areas indicate where the EQBO-WQBO differences are not statistically significant at the 99 % confidence level. The grey dashed contour stands for a zero difference.

The influence of the QBO on the stratospheric polar vortex is of particular importance since the vortex can have a direct effect on tropospheric weather patterns. As explained in the introduction, during an EQBO phase Rossby waves tend to get deflected poleward, thus weakening the vortex, whereas in a WQBO phase Rossby waves get deflected equatorward, reinforcing the vortex. Figure 9 depicts the zonal-mean zonal wind response to the QBO in the NH as differences between EQBO and WQBO phases. For the samples to be comparable, different thresholds were applied when selecting the QBO phases, retaining the 120 months showing minimum and maximum zonal-mean zonal wind values at 50 hPa to composite the EQBO and the WQBO phases respectively. In the tropics, the difference between QBO phases weakens as the radiative forcing intensifies, especially in CPL future. The extratropical response shows the expected weakening of the stratospheric vortex representing the Holton-Tan effect in the three experiments, with the largest dampening taking place in CPL future (Fig. 9c) and a slightly less intense weakening in CPL present when compared to CPL past (Fig. 9a-b). The larger impact observed in Fig. 9c could be related to an enhanced influence of the EQBO phase on the stratospheric vortex, while the WQBO effect appears to be weakened in the future experiment (Fig. 12e,f).

The effect on the extratropical circulation is well corresponded with the observed anomalies in the geopotential height field at 10 hPa (Fig. 10). In agreement with Fig. 9, CPL future shows the largest positive Z anomaly, with an increase of over 400 m, indicative of a severely weakened polar vortex (Fig. 10c). Both CPL past and present show positive Z anomalies with intensities that are also in good accord with the response observed in Fig. 9. In general, the impact on the polar vortex is annular, in good agreement to what is observed in reanalyses *Anstey and Shepherd* (2014) and in the previous EC-EARTH model version *Palmeiro et al.* (2020).

IV. CONCLUSIONS

In this work we have analyzed a set of 250-year long atmosphere-only and coupled simulations, performed with the state-of-the-art global climate model EC-EARTH, to assess radiatively-forced changes in the QBO and its teleconnection to the extratropical stratosphere under past, present and future conditions. A summary of the obtained results is outlined here.

1) Under a warming climate, i.e. future vs present/past, the QBO shows a marked acceleration in the downward progression of its phases, which translates into a shortening of its cycle. The acceleration is likely related to increased wave activity associated with enhanced deep tropical convection, following the arguments of *Taguchi* (2010). This impact of the radiative forcing is more clearly detectable in the coupled simulations, and can be linked to a significant warming (air temperature and SST) in the tropics.

2) Associated with the enhanced deep convection, an increased tropical upwelling through the tropopause is also expected (*Kawatani and Hamilton* 2013), leading to a weakening of the QBO amplitude in the lower strato-

sphere (*Richter et al.* 2020). Consistent with these arguments, our results from the coupled simulations show a clear weakening of the QBO wind regimes at lower-stratospheric levels.

3) Although the coupled simulation in a warming climate yields a shortening of the QBO period and a weakening of the QBO amplitude in the lower stratosphere, theses changes do not translate into a statistically significant modulation of the Holton-Tan effect on the polar vortex.

4) The atmosphere-only simulations, despite correctly simulating QBO variability and showing an acceleration of the QBO in future climate, as compared to past and present conditions, fail to consistently capture the expected impact of the radiative forcing on deep tropical convection and tropospheric temperature, as well as on the QBO amplitude.

5) Together, our results suggest that ocean-atmosphere coupling plays an important role in communicating the effect of the radiative forcing, particularly for future climate, to changes in the QBO period and amplitude, conceivably via enhancing deep tropical convection.

This work has mainly focused on the impact of the radiative forcing analysing separately atmosphere-only and coupled simulations, though a targeted assessment of how atmosphere-ocean coupling affects this impact would also be of interest and could serve as a starting point for future studies.

ACKNOWLEDGMENTS

First and foremost, I would like to express my deepest and most sincere gratitude to my supervisors, Froila Palmeiro Núñez and Javier García Serrano, for their invaluable guidance throughout the development of this work, for their endless patience and for the many hours of stimulating discussion on climate science and the world around research. I am also thankful to my master's colleagues for the good moments shared throughout this difficult year. Lastly, I am extremely grateful to my friends and family for their unconditional support through all these years.

REFERENCES

Anstey, J. A., and T. G. Shepherd, High-latitude influence of the quasi-biennial oscillation, *Quarterly Journal of the Royal Meteorological Society*, *140*(678), 1–21, 2014.

Anstey, J. A., T. P. Banyard, N. Butchart, L. Coy, P. A. Newman, S. Osprey, and C. Wright, Quasi-biennial oscillation disrupted by abnormal Southern Hemisphere stratosphere, *Earth and Space Science Open Archive*, p. 23, 2020.

Anstey, J. A., T. P. Banyard, N. Butchart, L. Coy, P. A. Newman, S. Osprey, and C. Wright, Prospect of increased disruption to the QBO in a changing climate, 2021.

Baldwin, M. P., The quasi-biennial oscillation, *Reviews of Geophysics*, *39*(2), 179–229, 2001.

Butchart, N., The Brewer-Dobson circulation, *52*(2), 157–184, 2014.

Butchart, N., et al., Overview of experiment design and comparison of models participating in phase 1 of the SPARC Quasi-Biennial Oscillation initiative (QBOi), *Geoscientific Model Development*, *11*(3), 1009–1032, 2018.

Döscher, R., et al., The EC-Earth3 Earth System Model for the Climate Model Intercomparison Project 6, *Geoscientific Model Development Discussions*, (February), 1–90, 2021.

Flury, T., D. L. Wu, and W. G. Read, Variability in the speed of the Brewer-Dobson circulation as observed by Aura/MLS, *Atmospheric Chemistry and Physics*, *13*(9), 4563–4575, 2013.

Holton, J. R., and G. J. Hakim, *An introduction to dynamic meteorology: Fifth edition*, vol. 9780123848, 1–532 pp., 2012.

Holton, J. R., and H.-C. Tan, The Influence of the Equatorial Quasi-Biennial Oscillation on the Global Circulation at 50 mb, *Journal of the Atmospheric Sciences*, 1980.

Kawatani, Y., and K. Hamilton, Weakened stratospheric quasibiennial oscillation driven by increased tropical mean upwelling, *Nature*, *497*(7450), 478–481, 2013.

Osprey, S. M., N. Butchart, J. R. Knight, A. A. Scaife, K. Hamilton, J. A. Anstey, V. Schenzinger, and C. Zhang, An unexpected disruption of the atmospheric quasi-biennial oscillation, *Science*, *353*(6306), 1424–1427, 2016.

Palmeiro, F. M., J. García-Serrano, O. Bellprat, P. A. Bretonnière, and F. J. Doblas-Reyes, Boreal winter stratospheric variability in EC-EARTH: High-Top versus Low-Top, *Climate Dynamics*, *54*(5-6), 3135–3150, 2020.

Plumb, R. A., A "tropical pipe" model of stratospheric transport, *Journal of Geophysical Research Atmospheres*, *101*(D2), 3957–3972, 1996.

Richter, J. H., J. A. Anstey, N. Butchart, Y. Kawatani, G. A. Meehl, S. Osprey, and I. R. Simpson, Progress in Simulating the Quasi-Biennial Oscillation in CMIP Models, *Journal of Geophysical Research: Atmospheres*, *125*(8), 1–14, 2020.

Taguchi, M., Observed connection of the stratospheric quasi-biennial oscillation with el niño–southern oscillation in radiosonde data, *Journal of Geophysical Research: Atmospheres*, *115*(D18), 2010.

APPENDIX

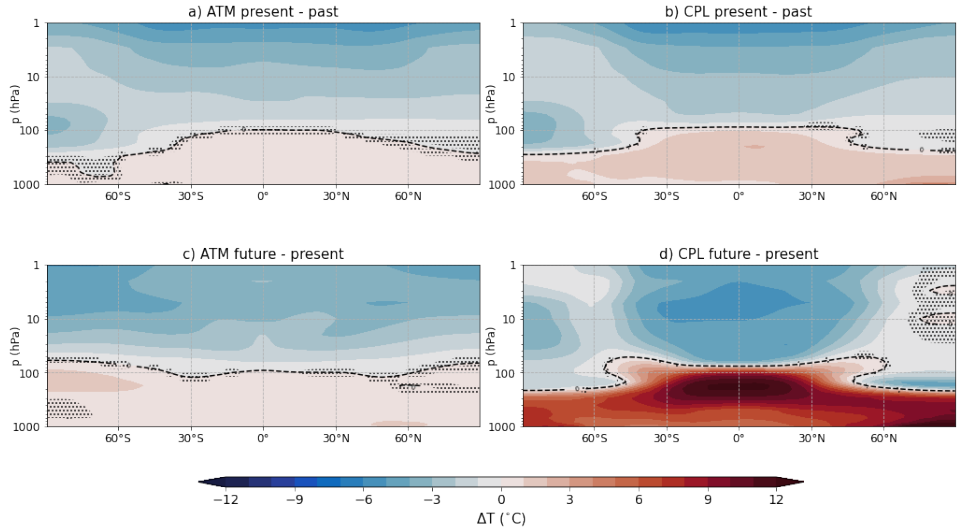

FIG. 11. Differences in zonally averaged air temperature between EC-EARTH simulations of the same family. Red and blue shading (every 1 °C) represents warmer and colder regions, respectively. Dotted areas indicate where the differences are not statistically significant at the 99 % confidence level. The black dashed contour line stands for 0 temperature difference.

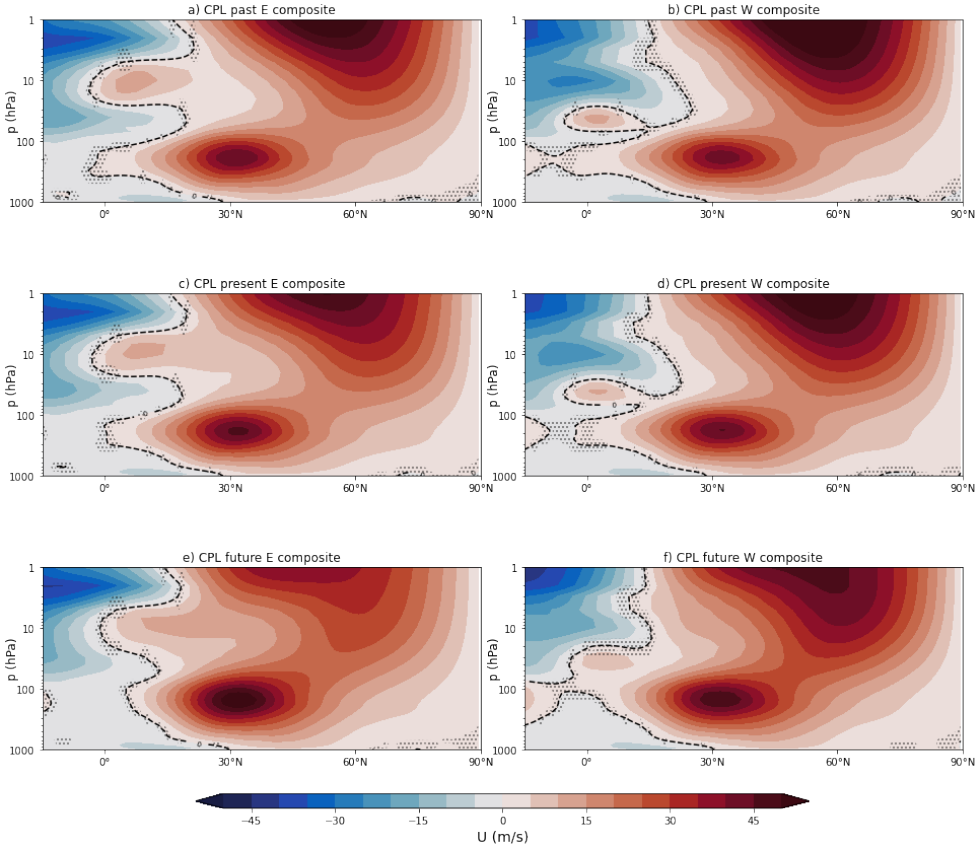

FIG. 12. Vertical cross-section of zonal-mean zonal wind composite, with EQBO on the left panels and WQBO on the right panels, identified with $\overline{U}_{EQ50}$, during boreal winter (DJF) for the EC-EARTH CPL simulations. Red and blue shading (every 5 ms^{-1}) represents westerly and easterly winds, respectively. Dotted areas indicate where the differences are not statistically significant at the 99 % confidence level. The black dashed contour line stands for a zero difference.

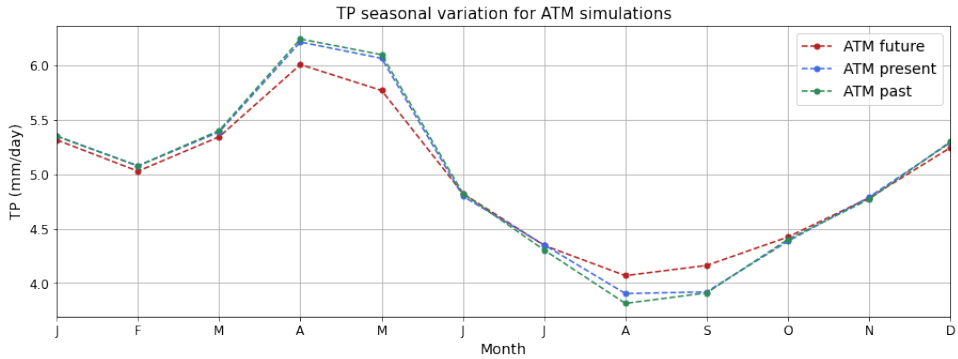

FIG. 13. Seasonal variation of the TP field for the ATM family, meridionally averaged over 5°S and 5°N.

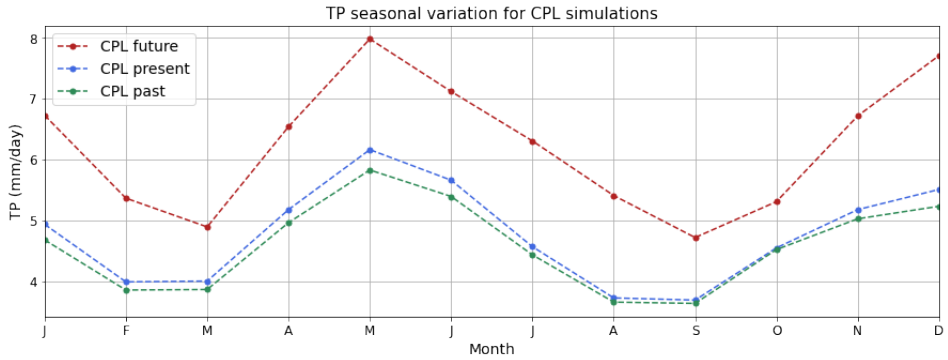

FIG. 14. Seasonal variation of the TP field for the CPL family, meridionally averaged over 5°S and 5°N.

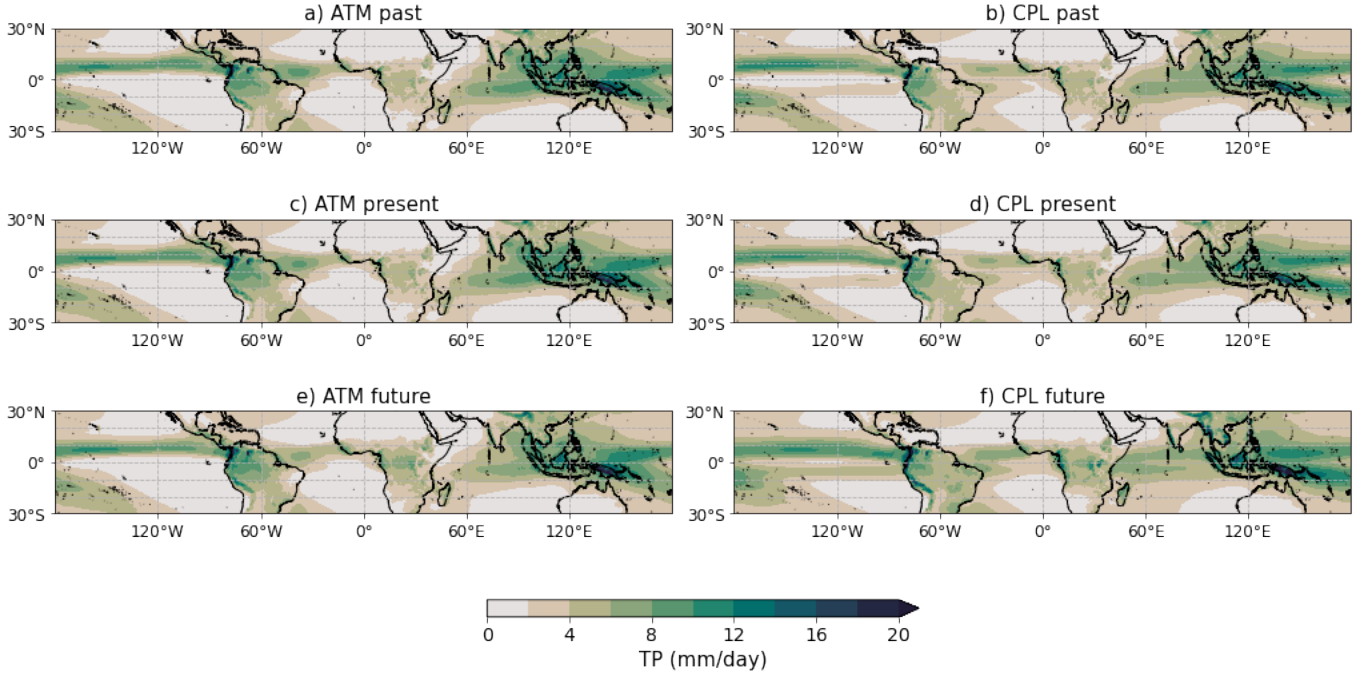

FIG. 15. Annual-mean TP climatology for the EC-EARTH simulations. Coloured shading (every 2 mm/day) represents increasingly higher precipitation rates.